ISSN 1068-7998, Russian Aeronautics, 2020, Vol. 63, No. 2, pp. 177–186. © Allerton Press, Inc., 2020.
Russian Text © The Author(s), 2020, published in Izvestiya Vysshikh Uchebnykh Zavedenii, Aviatsionnaya Tekhnika, 2020, No. 2, pp. 3–11.

STRUCTURAL MECHANICS AND STRENGTH OF FLIGHT VEHICLES

Calculation of Parameters for Manufacturing the Bearing Surfaces by Pressurization

R. Sh. Gimadiev[a], V. I. Khaliulin[b,*], and N. V. Levshonkov[b]

[a]*Kazan State Power Engineering University, ul. Krasnosel'skaya 51, Kazan, 420066 Tatarstan, Russia*

[b]*Tupolev Kazan National Research Technical University, ul. Karla Marksa 10, Kazan, 420111 Tatarstan, Russia*

**e-mail: pla.kai@mail.ru*

Received December 17, 2019; revised February 19, 2020; accepted February 19, 2020

Abstract—The statement and the technique of solving a new class of problems for calculating the process parameters of the manufacture of inflatable bearing surfaces of aircraft are proposed. The technique development is based on dependencies of interaction dynamics of the stretchable fabric with internal pressure in the wing cavity. The model takes into account the imbalance of the pressure and tension forces in the shell surface that initiate its high-frequency oscillation. The algorithms obtained allow predicting and then correcting the shape of the wing profile in accordance with the aerodynamics guidelines.

DOI: 10.3103/S1068799820020014

Keywords: inflatable wing, manufacturing technology, soft shell, wing shape calculation.

INTRODUCTION

Large dimensions of load-bearing lift surfaces cause certain inconveniences during an aircraft transportation, basing, and storage. Various transformable structures are used to improve portability, including folding wings [1] or helicopter blades [2], disk wings with retracting [3] or folding blades [4], etc.

Soft inflatable load-bearing aerodynamic surfaces ensure compactness of an aircraft during storage and transportation.

Aircraft with inflatable units are a separate class.

The first experiments with inflatable wing were carried out in the 1930s. These experiments were continued in 1956–1973 within the scope of the US military program aimed at the development of an inflatable aircraft with a weight of more than 300 kg.

The literature provides the examples of development and operation of manned aircraft of totally inflatable units [5], unmanned aerial vehicles [6], inflatable helicopter hulls, and paragliders [7]. There are also hybrid wings with a rigid front and inflatable rear part [8]. The subject of research is also the aerodynamics of the flow around the profile [9, 10], oscillations in the inflatable wing [11], and the assessment of the temperature effect on the inflatable wing properties [12, 13]. A number of aeroelastic and mechanical issues of the soft wing are considered in [14–25].

The most common technical solution is a multi-spar (multi-walled) wing [12], [6]. Sometimes, spars are tubular [6]. In a multi-walled structure, the straightness of generatrix lines of the surface along the wing span is easily implemented and the bending moment is well perceived. At the same time, another layer of fabric, which is mounted on top the inflatable system to ensure the smoothness of the surface, makes the design heavier. Besides, it is difficult to create the specific aerodynamic profile in the soft wing section. Thus, the ensuring the specific aerodynamic profile of an inflatable wing at the design stage remains a timely matter.

To determine the shape of the wing under pressurization, an algorithm is developed for numerical solution of the dynamic problem of elasticity using the finite difference method in an explicit scheme. In this case, the effect of interaction of the rib geometry and the local buckling of the wing element is taken into account. The stationary shape of the wing is defined as the ultimate solution of the dynamic problem. The required aerodynamic shape of the wing is determined on the basis of numerical experiments as a function of pressure.

STATEMENT OF THE PROBLEM

An inflatable wing is studied (Fig. 1). Skins, ribs, and spars are made of impermeable fabric impregnated with resin. The ribs are connected to the skin and the spars and determine the profile of the wing in their sections. The spars are connected to the ribs and have no connection with the skin. They take part of bearing of the bending moment and shear force. The force is transmitted to the spars from the ribs.

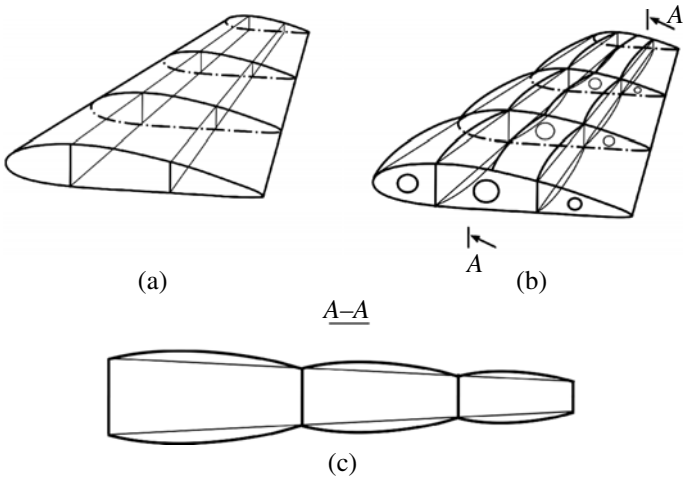

Fig. 1. Inflatable wing scheme: (a)—the nominal shape; (b)—the shape after pressurization; (c)—the longitudinal section.

The following processing scheme is suggested for manufacturing the wing. At the beginning, the fabric is impregnated with resin. Then, the shell with a soft frame is inflated until it acquires a geometry that meets aerodynamic requirements.

After that, the resin is cured under temperature or ultraviolet radiation exposition, depending on cure initiator. The result is a bearing surface with a hard skin and a frame.

During pressurization, for simplicity, we can neglect the deformation of the ribs and spars in the plane of their walls, as well as their deplanation, since the pressure on both sides is the same. At the same time, the skin is stretched as the pressure increases. Its surface between the ribs takes the shape of a doubly curved shell (Fig. 1b).

This work is aimed at creation of a technique that allows calculating the shape of convex fragments of the skin depending on the level of pressure inside it. This allows one to adjust the level of pressurization to obtain the profile specified by aerodynamics.

The theoretical foundations of developing such a technique are presented in [26–34]. These works describe open shells with flexible deformable linear reinforcements such as slings. The theory was applied in parachute systems.

This paper proposes the formulation of a new class of problems on creation of a methodology for calculating the process parameters of manufacturing the inflatable bearing surfaces of aircraft.

THE EQUATIONS OF DYNAMICS OF LOADING OF THE FABRIC SURFACE OF THE WING

The method proposed for determining the process parameters is based on the following: in pressurization, the equilibrium state of a shell fragment located between the ribs is established as a result of a dynamic process between internal pressure and forces in the fabric shell. This makes it necessary to consider the dynamics of soft shells under pressure. Shell fragments joined in the rib area are shown in Fig. 2.

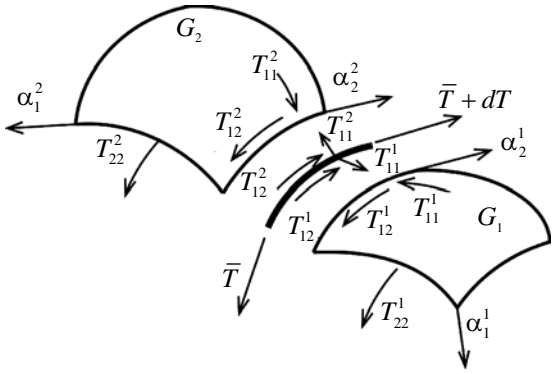

Fig. 2. Shell fragments under pressurization.

Let the surface and mass forces acting on the selected shell element be as follows:

$$\bar{P} = \bar{p}dF = \bar{p}\sqrt{g}\,d\alpha_1 d\alpha_2; \quad \bar{Q} = \bar{q}dF_0\rho_0 = \rho_0\bar{q}\sqrt{g_0}\,d\alpha_1 d\alpha_2,$$

where ρ_0 is the density of undeformed shell material; $\bar{q}$ is the density of mass force; $dF = \sqrt{g}\,d\alpha_1 d\alpha_2$ is the element of the surface under consideration.

In the theory of soft shells, one does not operate by stresses (forces per unit of area), but tensions (forces per unit of length). This is mainly due to the fact that the thickness of textile materials is a very vague concept and depends on the method of weaving, threads packing density, etc.

The following forces are applied to the elementary areas, limited by sections α_1 and α_2:

$$-\left(T_{11}\bar{\tau}_1 + T_{12}\bar{\tau}_2\right)\sqrt{g_{22}}\,d\alpha_2; \quad -\left(T_{21}\bar{\tau}_1 + T_{22}\bar{\tau}_2\right)\sqrt{g_{11}}\,d\alpha_1,$$

where, $\bar{\tau}_1$ and $\bar{\tau}_2$ are the unit vectors of the main basis vector; T_{ik} $(i,k=1,2)$ are the physical components of the membrane stress tensor.

We assume that mass forces include inertial forces. Given the d'Alembert principle, the equation of motion of the fabric shell can be written as

$$\rho_0\sqrt{g_0}\,\frac{\partial^2\bar{r}}{\partial t^2} = \frac{\partial}{\partial\alpha_1}\left(\left(T_{11}\bar{\tau}_1 + T_{12}\bar{\tau}_2\right)\sqrt{g_{22}}\right) + \frac{\partial}{\partial\alpha_2}\left(\left(T_{22}\bar{\tau}_2 + T_{21}\bar{\tau}_1\right)\sqrt{g_{11}}\right) + \bar{p}\sqrt{g} \; + \; \rho_0\bar{q}\sqrt{g_0}, \qquad (1)$$

where $\bar{r}$ is the radius vector of the point of the selected surface element in space, which determines the coordinates of the surface point in space at time t.

The wing rib splits the smooth shell into two subregions G_1 and G_2 (see Fig. 2). Let there be the tangent tensions T_{12}^1, T_{12}^2 and normal tensions T_{11}^1, T_{11}^2 on the boundaries of these subregions. Here, superscripts refer to subregions G_1 and G_2. Then, the equations of motion of each subregion are described by Eq. (1) with the boundary tensions T_{12}^1, T_{11}^1 and T_{12}^2, T_{11}^2, respectively, for these subregions and these tensions are determined as a result of mutual deformation of the shell elements G_1 and G_2 with the rib.

Thus, the dissected equations of motion of smooth shells are considered taking into account the boundary conditions.

THE EQUATIONS OF THE WING PRESSURIZATION IN THE CARTESIAN COORDINATE SYSTEM

Let the shell surface be assigned to the Cartesian system of orthogonal coordinates x_1, x_2, x_3 and given in parametric form

$$x_1 = x_1(\alpha_1, \alpha_2, t); \quad x_2 = x_2(\alpha_1, \alpha_2, t); \quad x_3 = x_3(\alpha_1, \alpha_2, t).$$

For the undeformed state of surface, the directions $\alpha_1 \wedge \alpha_2 = 90\,\text{deg}$ are selected.

The radius vector of any point on the surface can be represented as $\overline{r} = \sum_{k=1}^{3} x_k \overline{i}_k$, where $\overline{i}_k (k = 1,\ 2,\ 3)$ is the right triple of unit vectors. Further, we apply the summation convention for same subscripts, so $x_k \overline{i}_k = \sum_{k=1}^{3} x_k \overline{i}_k$.

Each surface point is associated with its local basis, and the main vectors of the bases are determined as $\overline{r}_j = \partial\, \overline{r} / \partial \alpha_j = r_{j,k} \overline{i}_k$.

Internal geometry of the surface is determined by its metric tensor. Its components are calculated using the following equation

$$g_{jm} = \frac{\partial\, \overline{r}}{\partial \alpha_j} \frac{\partial\, \overline{r}}{\partial \alpha_m} = r_{j,k} r_{m,k}, \quad j, m = 1, 2. \tag{2}$$

In Eq. (2), components with the same subscripts g_{11} and g_{22} are equal to the squares of the lengths of the main basis vectors $\overline{r}_1$ and $\overline{r}_2$. Their directions are determined using the cosines of the corresponding unit vectors $\overline{e}_1$ and $\overline{e}_2$. If $l_{jk} = \cos\left(\overline{e}_j, \overline{i}_k\right)$, then $\overline{e}_j = l_{jk} \overline{i}_k$.

To calculate the direction cosines l_{jk}, we express the unit vectors in terms of the main vectors $\overline{e}_j = \overline{r}_j \big/ \sqrt{g_{jj}}$. Then, the direction cosines are determined as follows

$$l_{jk} = r_{j,k} \big/ \sqrt{g_{jj}}, \quad j = 1,\ 2; \quad k = 1,\ 2,\ 3. \tag{3}$$

The unit normal to the surface is as follows

$$\overline{e}_3 = \overline{e}_1 \times \overline{e}_2 \sqrt{g_{11} g_{22}} \big/ \sqrt{g}. \tag{4}$$

The direction cosines of the normal to the surface are determined by the well-known equations

$$\begin{aligned} l_{31} &= \left(l_{12} l_{23} - l_{13} l_{22}\right) \sqrt{g_{11} g_{22}} \big/ \sqrt{g}; \\ l_{32} &= \left(l_{13} l_{21} - l_{11} l_{23}\right) \sqrt{g_{11} g_{22}} \big/ \sqrt{g}; \\ l_{33} &= \left(l_{11} l_{22} - l_{12} l_{21}\right) \sqrt{g_{11} g_{22}} \big/ \sqrt{g}. \end{aligned} \tag{5}$$

For writing the equation of motion in the Cartesian coordinate system, we use decomposition in directions of local basis $\overline{p} = p_k \overline{e}_k$ and $\overline{q} = q_k \overline{e}_k$.

Let the axis x_3 be vertical. Projecting Eq. (1) on the Cartesian axes and taking into account Eqs. (4) and (5), we obtain three scalar equations of motion:

$$\rho_0\sqrt{g_0}\frac{\partial^2 x_1}{\partial t^2}=\frac{\partial}{\partial\alpha_1}\left(\left(T_{11}l_{11}+T_{12}l_{21}\right)\sqrt{g_{22}}\right)+\frac{\partial}{\partial\alpha_2}\left(\left(T_{22}l_{22}+T_{21}l_{11}\right)\sqrt{g_{11}}\right)$$

$$+p_3\left(l_{12}l_{23}-l_{13}l_{22}\right)\sqrt{g_{11}g_{22}}\ +\left(p_1l_{11}+p_2l_{21}\right)\sqrt{g}\ ;$$

$$\rho_0\sqrt{g_0}\frac{\partial^2 x_2}{\partial t^2}=\frac{\partial}{\partial\alpha_1}\left(\left(T_{11}l_{12}+T_{12}l_{22}\right)\sqrt{g_{22}}\right)+\frac{\partial}{\partial\alpha_2}\left(\left(T_{22}l_{22}+T_{21}l_{12}\right)\sqrt{g_{11}}\right)$$

$$+p_3\left(l_{13}l_{21}-l_{11}l_{23}\right)\sqrt{g_{11}g_{22}}\ +\left(p_1l_{12}+p_2l_{22}\right)\sqrt{g}\,; \tag{6}$$

$$\rho_0\sqrt{g_0}\frac{\partial^2 x_3}{\partial t^2}=\frac{\partial}{\partial\alpha_1}\left(\left(T_{11}l_{13}+T_{12}l_{23}\right)\sqrt{g_{22}}\right)+\frac{\partial}{\partial\alpha_2}\left(\left(T_{22}l_{23}+T_{21}l_{13}\right)\sqrt{g_{11}}\right)$$

$$+p_3\left(l_{11}l_{22}-l_{12}l_{21}\right)\sqrt{g_{11}g_{22}}\ +\left(p_1l_{13}+p_2l_{23}\right)\sqrt{g}\ -\rho_0 q\sqrt{g_0}\,.$$

Apart from three equations of motion, the system of resolving equations contains

—geometric relations

$$g_{jm}=\frac{\partial\overline{r}}{\partial\alpha_j}\frac{\partial\overline{r}}{\partial\alpha_m}=r_{j,k}r_{m,k},\quad j,m=1,2; \tag{7}$$

—relations for the physical components of the strain tensor

$$\varepsilon_{ik}=\frac{g_{ik}-g_{ik}^0}{2\sqrt{g_{ii}^0g_{kk}^0}}; \tag{8}$$

—relations for degrees of deformation $\lambda_i=\sqrt{1+2\varepsilon_{ii}}$, $(i=1,2)$ and the shear angle

$$\sin\theta=2\varepsilon_{12}\big/\left(\lambda_1\lambda_2\right). \tag{9}$$

Parameter ε_{12} characterizes the angle of shift between coordinate lines α_1 and α_2 in deformed condition.

Textile materials have a low shear stiffness, about 2 % compared to the tensile stiffness. Therefore, the shear moduli may be considered as $E_{12}=E_{21}=0$. Then, the physical relations for the fabric as applied to Eqs. (6) may be as follows

$$\begin{aligned}T_{11}&=\left(E_{11}e_{11}+\nu_{21}E_{22}e_{22}\right)\big/\left(1-\nu_{12}\nu_{21}\right)+\eta\dot{e}_{11}\,;\\ T_{22}&=\left(E_{22}e_{22}+\nu_{12}E_{11}e_{11}\right)\big/\left(1-\nu_{12}\nu_{21}\right)+\eta\dot{e}_{22}\,,\end{aligned} \tag{10}$$

where $\nu_{12}=\nu_{21}=0.25$ are the analogues to the Poisson's ratio; e_{11},e_{22} are the elongations; $\dot{e}_{11}$ and $\dot{e}_{22}$ are the elongation rates; η is the coefficient of viscous friction in the material; E_{11},E_{22} are the tensile moduli.

During pressurization, the pressure and tension forces are unbalanced. As a result, when the shell is pressurized, there is a high-frequency oscillation of the shell elements. Oscillation of the shell itself affects the value of the effective pressure. When the shell element moves against the internal pressure, the pressure acting on this element increases, and decreases for the opposite direction of motion, i.e. the inflation is dampened by oscillation of the shell.

When the shell is pressurized, the overpressure $p(t)$ is approximated by the following equation

$$p(t)=\tilde{p}(t)\left(1-\nu^nV^n\right)^2\operatorname{sgn}\left(1-\nu^nV^n\right) \tag{11}$$

that is used in the theory of soft shells in studying the dynamics of parachutes [34].

The term $\nu^n V^n$ is introduced into Eq. (11), where ν^n is the aerodynamic damping coefficient of the medium when the shell moves in this medium with the rate $V^n = \partial u_3 / \partial t$ to the normal $\bar{e}_3$ to the surface. Here, u_3 is the component of the shell displacement vector to the surface normal. In Eq. (11), the law of the distribution of excess pressure $\tilde{p}$ over spatial coordinates α^1, α^2 is assumed to be determined at time *t*.

Further, let us consider that when $t = t_0$, the initial shape of the shell σ_0 is described as

$$r\left(\alpha^1, \alpha^2, t_0\right) = r\left(\alpha^1, \alpha^2\right),$$

where α^1 is the curvilinear coordinate along the generatrix of the shell varying within $0 \le \alpha^1 \le l_1$ and α^2 is the circumferential coordinate varying within $0 \le \alpha^2 \le l_2$.

THE DIFFERENCE SCHEME FOR SOLVING THE PROBLEM

A significant number of works have been devoted to the calculation of reinforced shells [35–41]. This paper supposes the difference scheme for solving the problem.

The calculated element (*i, j*) (Fig. 3) of the difference grid covering the deformed surface is being considered. It is assumed that the mass of the hatched element is concentrated in the node (*i, j*) (Fig. 3a). In this case, the difference grid in general will be deplaned (Fig. 3b). Let the triangles *OAB*, *OBC*, *OCD*, *ODE*, *OEF*, *OFK*, *OKL*, and *OLA* remain flat during deformation.

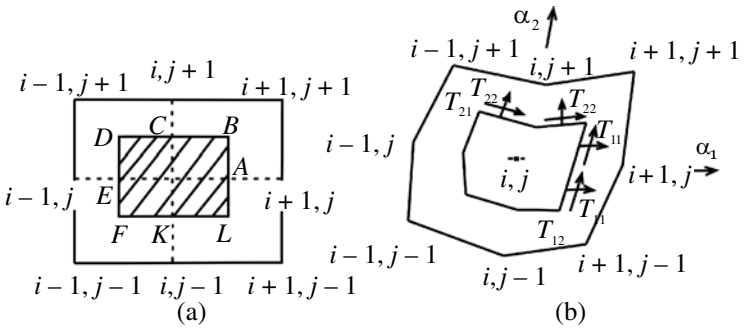

Fig. 3. Calculated elements: (a)—the hatch element of difference grid; (b)—the deplanation of the difference grid.

At each point of time, the elongation ratios in the directions α^1 and α^2 are calculated using the following equations:

$$\lambda_1^{i+1/2,j} = h_1^{-1}\left(\sum_{\gamma=1}^{3}\left(x_{i+1,j}^{\gamma} - x_{i,j}^{\gamma}\right)^2\right)^{1/2};$$

$$\lambda_2^{i,j+1/2} = h_2^{-1}\left(\sum_{\gamma=1}^{3}\left(x_{i,j+1}^{\gamma} - x_{i,j}^{\gamma}\right)^2\right)^{1/2};$$

$$\lambda_1^{i+1/2,j+1/2} = \left(\lambda_1^{i+1/2,j+1} + \lambda_1^{i+1/2,j}\right)/2;;$$

$$\lambda_2^{i+1/2,j+1/2} = \left(\lambda_2^{i+1,j+1/2} + \lambda_2^{i,j+1/2}\right)/2. \qquad (12)$$

where $h_1 = h_1(i,j)$ and $h_2 = h_2(i,j)$ are the distances between points $(i+1/2, j), (i, j+1/2)$ of the difference grid.

To calculate the direction cosines of the main basis vectors, the following relations are used:

$$\left\{l_{1,\gamma}\right\}\Big|_j^i = \frac{x^\gamma_{i+1,j} - x^\gamma_{i,j}}{h_1 \lambda_1^{i+1/2,j}}; \quad \left\{l_{2,\gamma}\right\}\Big|_i^j = \frac{x^\gamma_{i,j+1} - x^\gamma_{i,j}}{h_2 \lambda_2^{i,j+1/2}}. \tag{13}$$

Equations of motion (6) are associated with their difference analogues. For example, for $2 \le i \le n_1 - 1$; $2 \le j \le n_2 - 1$

$$\begin{aligned}\left\{V^\gamma\right\}_{i,j}^{n+1/2} = \left\{V^\gamma\right\}_{i,j}^{n-1/2} + P_{i,j}\frac{\Delta t}{h_1 h_2}F^\gamma_{i,j} + \frac{\Delta t}{\rho_0}\Bigg(\Big[\left\{T_{11}\lambda_2\right\}_{j+1/2}^{i+1/2}\left\{l_{1\gamma}\right\}_{j+1/2}^{i} + \left\{T_{11}\lambda_2\right\}_{j-1/2}^{i+1/2}\left\{l_{1\gamma}\right\}_{j-1/2}^{i} \\ - \left\{T_{11}\lambda_2\right\}_{j+1/2}^{i-1/2}\left\{l_{1\gamma}\right\}_{j+1/2}^{i-1} - \left\{T_{11}\lambda_2\right\}_{j-1/2}^{i-1/2}\left\{l_{1\gamma}\right\}_{j-1/2}^{i-1}\Big]\Big/(2h_1) + \Big[\left\{T_{22}\lambda_1\right\}_{i+1/2}^{j+1/2}\left\{l_{2\gamma}\right\}_{i+1/2}^{j} \\ + \left\{T_{22}\lambda_1\right\}_{i-1/2}^{j+1/2}\left\{l_{2\gamma}\right\}_{i-1/2}^{j} - \left\{T_{22}\lambda_1\right\}_{i+1/2}^{j-1/2}\left\{l_{2\gamma}\right\}_{i+1/2}^{j-1} - \left\{T_{22}\lambda_1\right\}_{i-1/2}^{j-1/2}\left\{l_{2\gamma}\right\}_{i-1/2}^{j-1}\Big]\Big/(2h_2) + \Delta t\ q_\gamma\Bigg).\end{aligned} \tag{14}$$

For Eq. (14), for example,

$$\left\{l_{1\gamma}\right\}_{j-1/2}^{i+1/2} = \left(x^\gamma_{i+1,j-1/2} - x^\gamma_{i,j-1/2}\right)\Big/\left(h_1\lambda^1_{i+1/2,j-1/2}\right)$$

and $F^\gamma_{i,j}$ is the sum of the projections of the areas of eight triangles adjacent to the node (i,j) on the plane $x^\gamma = 0$ $(\gamma = 1,2,3)$. So, for the first triangle

$$F^1_{i,j} = \frac{1}{2}\left(x^2_{i,j}\left(x^3_{i+1/2,j} - x^3_{i+1/2,j+1/2}\right) + x^2_{i+1/2,j}\left(x^3_{i+1/2,j+1/2} - x^3_{i,j}\right) + x^2_{i+1/2,j+1/2}\left(x^3_{i,j} - x^3_{i+1/2,j}\right)\right). \tag{15}$$

The projections of areas on the other planes $x^2 = 0$ and $x^3 = 0$ are determined in the same way. Moreover, the subscripts 1, 2, 3 change by a cyclic rearrangement.

The integration step is selected in accordance with the Courant–Friedrichs–Levy criterion

$$\Delta t < \alpha_k \min\left(h_1, h_2\right)/c, \tag{16}$$

where α_k is the Courant coefficient; c is the velocity of small disturbance propagation in the material (sound speed).

The boundary conditions for the shell are ensured on an extended grid, the dimensions of which are determined by the numbers $1, n_1$ and $1, n_2$. Subscripts i and j vary within $1 \le i \le n_1$, $1 \le j \le n_2$. The desired coordinates of the nodal points of the shell on the time layers are determined as follows

$$\left(x^\gamma\right)_{i,j}^{n+1} = \left(x^\gamma\right)_{i,j}^{n+1} + \Delta t\left(\tilde{V}^\gamma\right)_{i,j}^{n+1/2}, \quad \gamma = 1,2,3. \tag{17}$$

Thus, an explicit scheme of the finite difference method is used to generate a numerical solution of the formulated problem. As a result, in constructing a solution to the compiled system of equations, a discrete region is introduced $S_{n_i} = n_i h_i$, $n_i = 1,2,3...$, $S_i/\Delta s_i$ and $t_n = n\Delta t$, $n = 1,2,...$, $t/\Delta t - 1$.

In this case, the values of the desired functions at each integration step are determined through their known values at the previous step within a single end-to-end calculation algorithm.

The choice of coefficient of viscous friction η (10), the aerodynamic damping coefficient ν^n (11), the Courant coefficient α_k is based on numerical experiment.

Thus, based on algorithm (5)–(17), dynamic problems of deformation of soft-shell structures are solved by the finite different method in the explicit scheme. This algorithm provides a possibility to reduce the problem to an equilibrium deformed state. In this case, the pressure inside the wing and surface tension are balanced, and the shape of the wing is determined by specified internal pressure and design features.

The calculated surface shape is compared to the guidelines of aerodynamic calculation. It provides a possibility to make adjustments to the pressurization parameters to achieve the most rational shape of the airfoil.

CONCLUSIONS

The technology of manufacturing bearing surfaces such as a wing or wing mechanization by pressurization of soft impenetrable shell impregnated with the resin is considered.

The technique is proposed for calculating the buckling mode of inflated soft skin fragments located between the ribs. It provides a possibility to predict the configuration of the wing profile in all its sections and determine the necessary pressure to ensure rational aerodynamic properties. After pressurization, the shape of the wing is fixed by curing the resin under heat treatment or ultraviolet radiation.

REFERENCES

1. Ruzhitskii, E.I., *Sovremennaya aviatsiya: Amerikanskie samolety vertikal'nogo vzleta i posadki* (Modern Aviation: The American Vertical Takeoff and Landing Aircraft), Moscow: Astrel', 2000.
2. Ruzhitskii, E.I., *Vertolety* (Helicopters), Moscow: Viktoriya, AST, 1997.
3. Pavlov, V.A., Privalov, L.V., and Rybakov, A.V., RU Patent 2005655, *Byul. Izobr.*, 1994.
4. Pavlov, V.A. and Pavlov, V.V., Pavlov's Disk Wings, *Tekhnika – Molodezhi*, 2004, no. 4, pp. 28–29.
5. Inflatoplane, URL: http://www.airwar.ru/enc/xplane/inflatoplane.html.
6. Simpson, A.D., Design and Evaluation of Inflatable Wings for UAVs, *Doctoral Dissertation*, University of Kentucky, 2008, URL: https://uknowledge.uky.edu/gradschool_diss/589.
7. Pavlov, V.V., *Letatel'nye apparaty s preobrazuemym v nesushchii vint krylom* (Aircraft with a Convertible Wing), Kazan: Izd. KNITU-KAI, 2019.
8. Ortamevzi, G. and Zinchenko, D.N., Research of Aerodynamic Characteristics of Hybrid Wing, *Mekhanika Giroskopichnikh Sistem*, 2014, no. 28, pp. 131–139.
9. Folkersma, M., Schmehl, R., and Viré, A., Boundary Layer Transition Modeling on Leading Edge Inflatable Kite Airfoils, *Wind Energy*, 2019, vol. 22, issue 7, pp. 908–921.
10. Ortamevzi, G. and Zinchenko, D.N., Aerodynamic Characteristics of the Experimental Flying Model with a Hybrid Soft Skin Surface, *Mekhanika Giroskopichnikh Sistem*, 2015, no. 29, pp. 53–63.
11. Liu, L., Wang, D., and Yang, H., Study on Modal Properties of Flexible Inflatable Wing Skin Film Structure, *Journal of Physics: Conference Series*, 2018, vol. 1053, article no. 012041.
12. Liu, L., Hu, F., Jiang, Zh., Liu, T., and Xu, Y., Study on Influence of Ambient Temperature on Biaxial Stress and Strength of Flexible Inflatable Wing Film, *Results in Physics*, 2019, vol. 12, pp. 85–93.
13. Konyukhov, A.V. and Konoplev, Yu.G., Thermohyperelasticity Model and Its Application to the Study of Inflated Plate Instability. II, *Izv. Vuz. Av. Tekhnika*, 2006, no. 4, pp. 7–13 [Russian Aeronautics (Engl. Transl.), 2006, vol. 49, no. 4].
14. Gimadiev, R.Sh. and Dribnoi, V.I., Soft Wing Interaction with Incompressible Fluid Flow, *Trudy seminara Kazanskogo fiz.-tekhn. instituta Kazanskogo filiala AN SSSR* (Proc. of the Workshop of Kazan Institute of Physics and Technics, Kazan Branch of Science Academy of USSR), Kazan, 1981, no. 14, pp. 163–169.
15. Gimadiev, R.Sh. and Il'gamov, M.A., Continuous Potential Flow around the Soft Wing, *Trudy seminara Kazanskogo fiz.-tekhn. instituta Kazanskogo filiala AN SSSR "Gidrouprugost' obolochek"* (Proc. of the Workshop of Kazan Institute of Physics and Technics, Kazan Branch of Science Academy of USSR "Hydroelasticity of Shells"), Kazan, 1983, no. 16, pp. 43–52.
16. Gimadiev, R.Sh. and Il'gamov, M.A., Static Interaction of a Soft Wing Profile with Incompressible Fluid Flow, *Izv. Vuz. Av. Tekhnika*, 1998, no. 1, pp. 43–48 [Russian Aeronautics (Engl. Transl.), 1998, vol. 41, no. 1, pp. 38–43].
17. Bondar', V.S., Abashev, D.R., and Petrov, V.K., Plasticity of Materials under Proportional and Nonproportional Cyclic Loading, *Vestnik PNIPU. Mekhanika*, 2017, no. 3, pp. 53–74.

18. Bondar', V.S., Danshin, V.V., and Alkhimov, D.A., Analysis on Cyclic Deformation and Low-High-Cycle Fatigue in Uniaxial Stress State, *Vestnik PNIPU. Mekhanika*, 2016, no. 4, pp. 52–71.
19. Gilev, V.G., Rusakov, S.V., Pestrenin, V.M., and Pestrenina, I.V., Estimation of the Cylindrical Composite Shell Stiffness at the Initial Stage of Curing During Deployment by Internal Pressure, *Vestnik PNIPU. Mekhanika*, 2018, no. 1, pp. 93–99.
20. Pestrenin, V.M., Pestrenina, I.V., Rusakov, S.V., Kondyurin, A.V., and Korepanova, A.V., Packaging and Deployment of Large Shell Structures by Internal Pressure Loading, *Vestnik PNIPU. Mekhanika,* 2016, no. 4, pp. 303–316.
21. Pestrenin, V.M., Pestrenina, I.V., Rusakov, S.V., and Kondyurin, A.V., Packaging and Deployment of Large Shell Composite Structures by Internal Pressure Loading in Space, *Aerokosmicheskaya Tekhnika, Vysokie Tekhnologii i Innovatsii*, 2016, vol. 1, pp. 261–264.
22. Badriev, I.B., Makarov, M.V., and Paimushin, V.N., Numerical Investigation of a Physically Nonlinear Problem of Longitudinal Bending of Sandwich Plate with Transversal-Soft Core, *Vestnik PNIPU. Mekhanika*, 2017, no. 1, pp. 39–51.
23. Baryshev, A.A., Lychev, S.A., and Manzhirov, A.V., The Equilibrium Equations of Shells in the Coordinates of the General Form, *Izvestiya Saratovskogo Universiteta. Novaya seriya. Seriya: Matematika. Mekhanika. Informatika*, 2013, vol. 13, no. 2-1, pp. 44–53.
24. Lychev, S.A. and Baryshev, A.A., Equilibrium Equations for Material Uniform and Inhomogeneous Laminated Shells, *Vestnik PNIPU. Mekhanika*, 2012, no. 4, pp. 42–65.
25. Gimadiev, R.Sh., Gimadieva, T.Z., and Paimushin, V.N., The Dynamic Process of the Inflation of Thin Elastomeric Shells under the Action of an Excess Pressure, *Prikladnaya Matematika i Mekhanika*, 2014, vol. 78, issue 2, pp. 236–248 [J. of Applied Mathematics and Mechanics (Engl. Transl.), vol. 78, issue 2, pp. 163–171].
26. Gimadiev, R.Sh., About the Issue of Soft Shell Filling Dynamics, in *Modelirovanie dinamicheskikh protsessov v sploshnykh sredakh* (Modeling of Dynamic Processes in Continuous Media), Kazan: Institut Mekhaniki i Mashinostroeniya KazNTs RAN, 1997, pp. 81–87.
27. Gimadiev, R.Sh., Numerical Simulation of Soft Two-Shell Wing Deployment, *Vychislitel'nye Tekhnologii*, 1995, vol. 4, no. 11, pp. 51–59.
28. Gimadiev, R.Sh., Braking of a Body by a Soft Inflatable Shell on Impact on a Surface, *Izvestiya RAN. Mekhanika Tverdogo Tela*, 2017, no. 5, pp. 109–121.
29. Morozov, V.I., Ponomarev, A.T., and Rysev, O.V., *Matematicheskoe modelirovanie slozhnyh aerouprugih system* (Mathematical Simulation of Complex Aeroelastic Systems), Moscow: Fizmatlit, 1995.
30. Giniyatullin, A.G. and Gimadiev, R.Sh., Examining Balloon Catheters Sheath Filling in Inflation, *Meditsinskaya Tekhnika*, 1993, issue 2, pp. 30–33.
31. Gimadiev, R.Sh., Mathematical Modeling of Soft Wing Shape and Layout, *Izv. Vuz. Av. Tekhnika*, 1997, no. 3, pp. 79–83 [Russian Aeronautics (Engl. Transl.), 1997, vol. 40, no. 3, pp. 76–81].
32. Ridel', V.V., and Gulin, B.V., *Dinamika myagkikh obolochek* (Dynamics of Soft Shells), Moscow: Nauka, 1990.
33. Il'gamov, M.A., *Vvedenie v nelineinuyu gidrouprugost'* (Introduction to Nonlinear Hydroelasticity), Moscow: Nauka, 1991.
34. Gimadiev, R.Sh., *Dinamika myagkikh obolochek parashyutnogo tipa* (Dynamics of Soft Parachute-Type Shells), Kazan: KGEU, 2006.
35. Antuf'ev, B.A., Dynamics of a Discretely Reinforced Cylindrical Shell under Live Load, *Izv. Vuz. Av. Tekhnika*, 2016, no. 3, pp. 8–12 [Russian Aeronautics (Engl. Transl.), 2016, vol. 59, no. 3, pp. 303–307].
36. Iskenderov, R.A., and Amirova, R.A., Investigation of the Influence of Preliminary Buckling for a Reinforced Medium-Filled Cylindrical Shell on Critical Stresses of Overall Instability, *Izv. Vuz. Av. Tekhnika*, 2010, no. 4, pp. 67–69 [Russian Aeronautics (Engl. Transl.), 2010, vol. 53, no. 4, pp. 470–474].
37. Zheleznov, L.P., Kabanov, V.V., and Boiko, D.V., Nonlinear Deformation and Stability of Discrete-Reinforced Elliptical Cylindrical Composite Shells under Torsion and Internal Pressure, *Izv. Vuz. Av. Tekhnika*, 2018, no. 2, pp. 27–34 [Russian Aeronautics (Engl. Transl.), 2018, vol. 61, no. 2, pp. 175–182].
38. Dzhabrailov, A.Sh., Klochkov, Yu.V., Nikolaev, A.P., and Fomin, S.D., Analysis of Stresses in Branched Shells of Revolution with Joint Zones Using Triangular Finite Elements with Allowance for Elastoplastic

Deformation, *Izv. Vuz. Av. Tekhnika*, 2015, no. 1, pp. 8–13 [Russian Aeronautics (Engl. Transl.), 2015, vol. 58, no. 1, pp. 7–14].

39. Zheleznov, L.P., Kabanov, V.V., and Boiko, D.V., Nonlinear Deformation and Stability of Discretely Reinforced Elliptical Cylindrical Shells under Transverse Bending and Internal Pressure, *Izv. Vuz. Av. Tekhnika*, 2014, no. 2, pp. 8–13 [Russian Aeronautics (Engl. Transl.), 2014, vol. 57, no. 2, pp. 118–126].
40. Abdyushev, A.A., The Principle of Constructing a Computation Model of Equilibrium Ribbed Stiffened Shells in Linear Displacement-Based FEM Analysis, *Izv. Vuz. Av. Tekhnika*, 2013, no. 2, pp. 8–14 [Russian Aeronautics (Engl. Transl.), 2013, vol. 56, no. 2, pp. 111–125].
41. Zheleznov, L.P., Kabanov, V.V., and Boiko, D.V., Nonlinear Deformation and Stability of Supported Oval Cylindrical Shells under Torsion and Bending with Internal Pressure, *Izv. Vuz. Av. Tekhnika*, 2010, no. 4, pp. 64–66 [Russian Aeronautics (Engl. Transl.), 2010, vol. 53, no. 4, pp. 466–469].